Supplementary Information (SI) for Journal of Materials Chemistry C.


# ESI

## Low oxygen content β-SiAlON ceramics derived from polysilazane as host materials for blue-emitting $Ce^{3+}$-based phosphors

M. Kumari,[a] B. Tolve-Granier,[a] T. Hayakawa,[b] C. Gervais,[c] P. Carles,[a] Y. Iwamoto,[b] P. Thomas,[a] O. Masson,[a] S. Bernard*[a]

a. IRCER, CNRS, Univ. Limoges, Limoges, France.

b. Dept. Of life science and applied chemistry, Nagoya Institute of Technology, Japan

c. Sorbonne Université, CNRS, Laboratoire de Chimie de la Matière Condensée de Paris, 4 Place de Jussieu, 75005 Paris, France

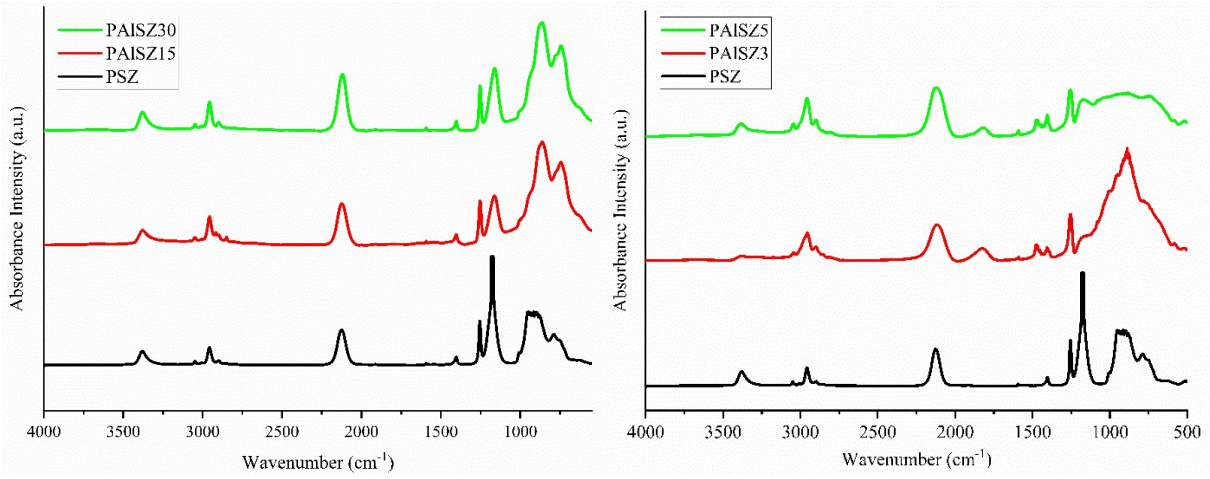


**Figure 1SI.** FTIR-ATR spectroscopy of the polymers: spectra for (a) liquid PAlSZX ($30 \leq X \leq 15$) and (b) for solid compounds: PAlSZX ($5 \leq X \leq 3$).

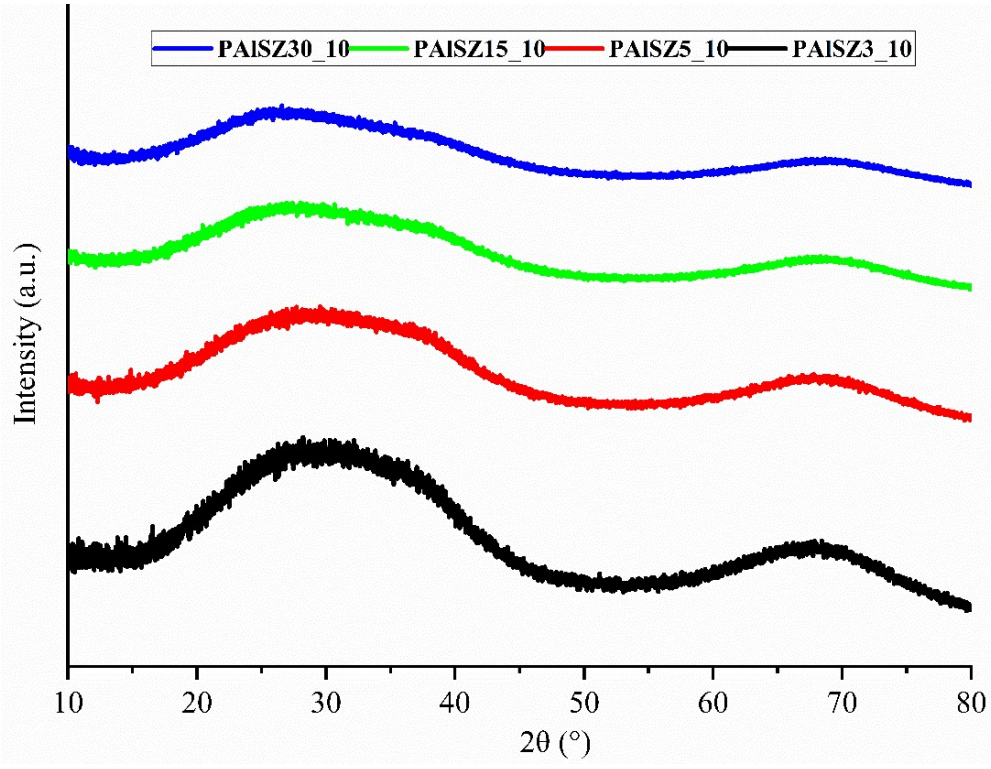


**Figure 2SI.** XRD patterns of PAlSZX_10 samples ($3 \leq X \leq 30$).

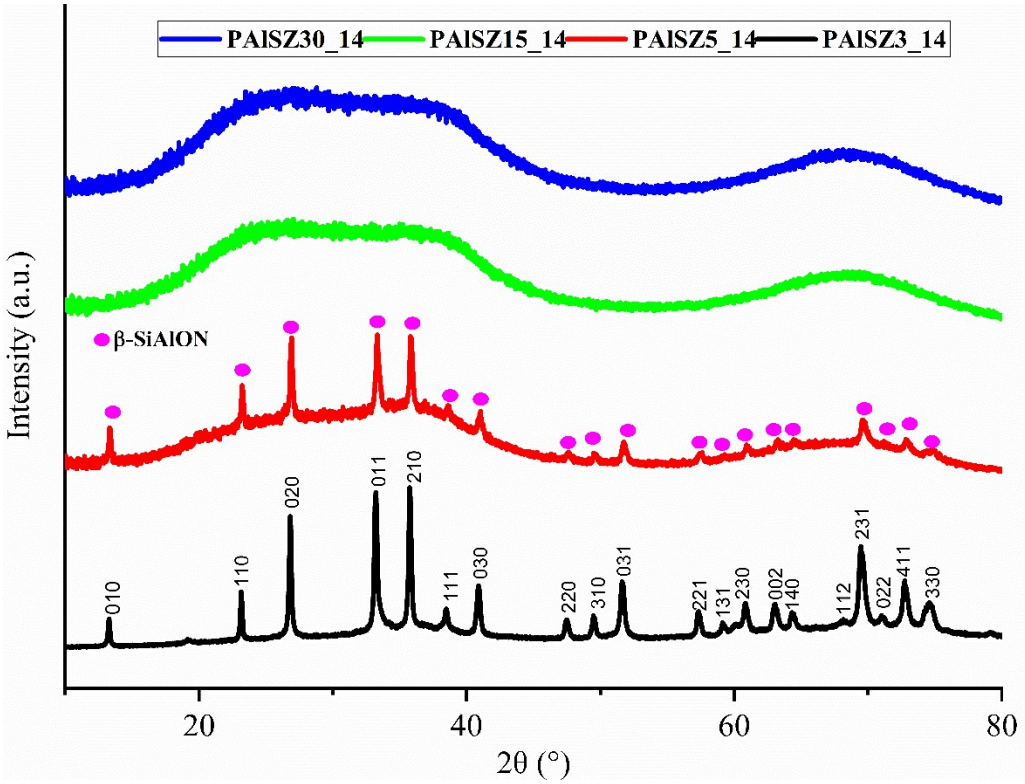


**Figure 3SI.** XRD patterns of PAlSZX_14 samples (3 ≤ X ≤ 30). *β-SiAlON Peak assignements are given for the **PAlSZ3_14** sample.*

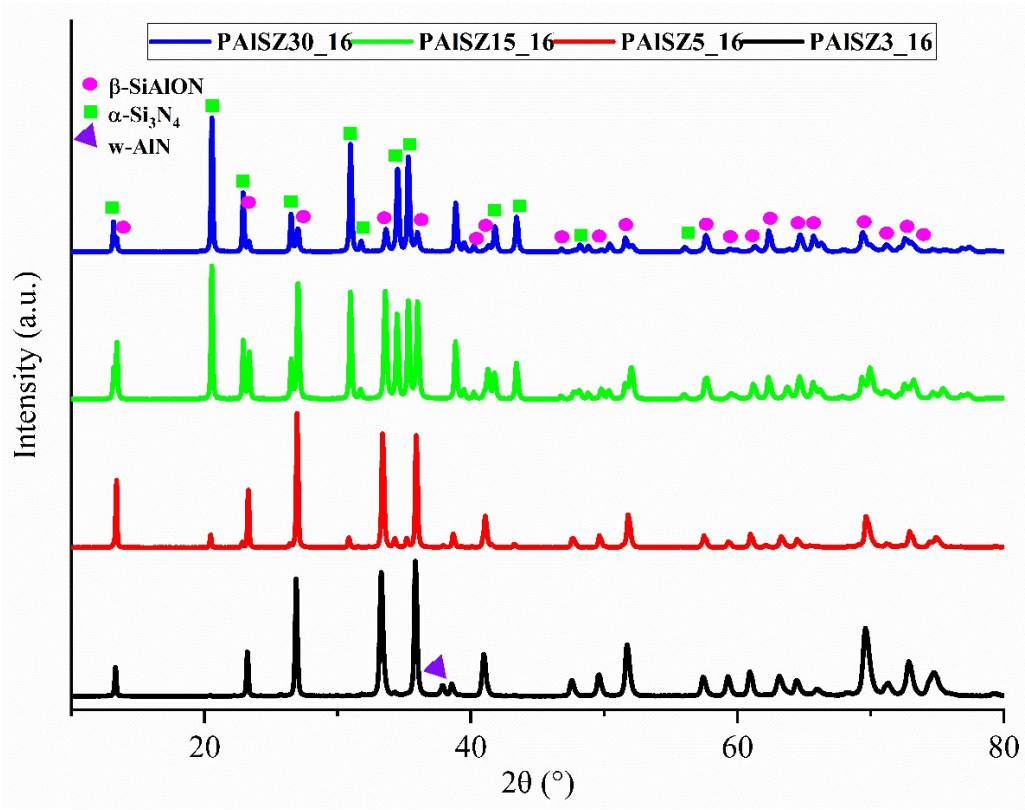


**Figure 4SI.** XRD patterns of PAlSZX_16 samples (3 ≤ X ≤ 30).

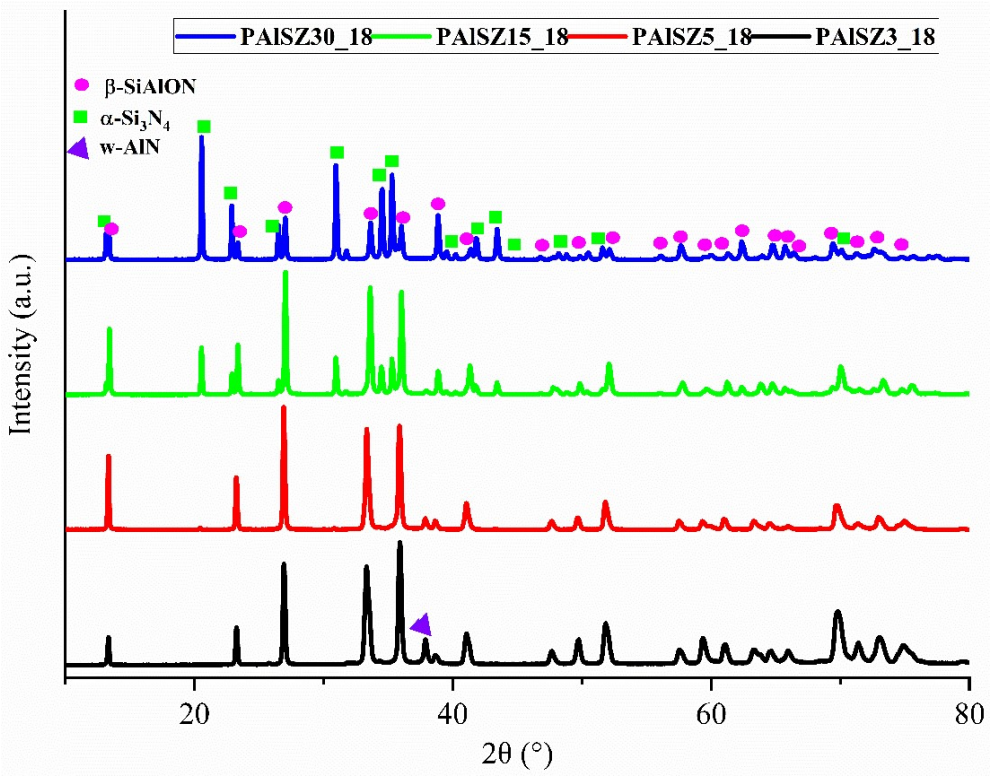


**Figure 5SI.** XRD patterns of PAlSZX_18 samples ($3 \leq X \leq 30$).

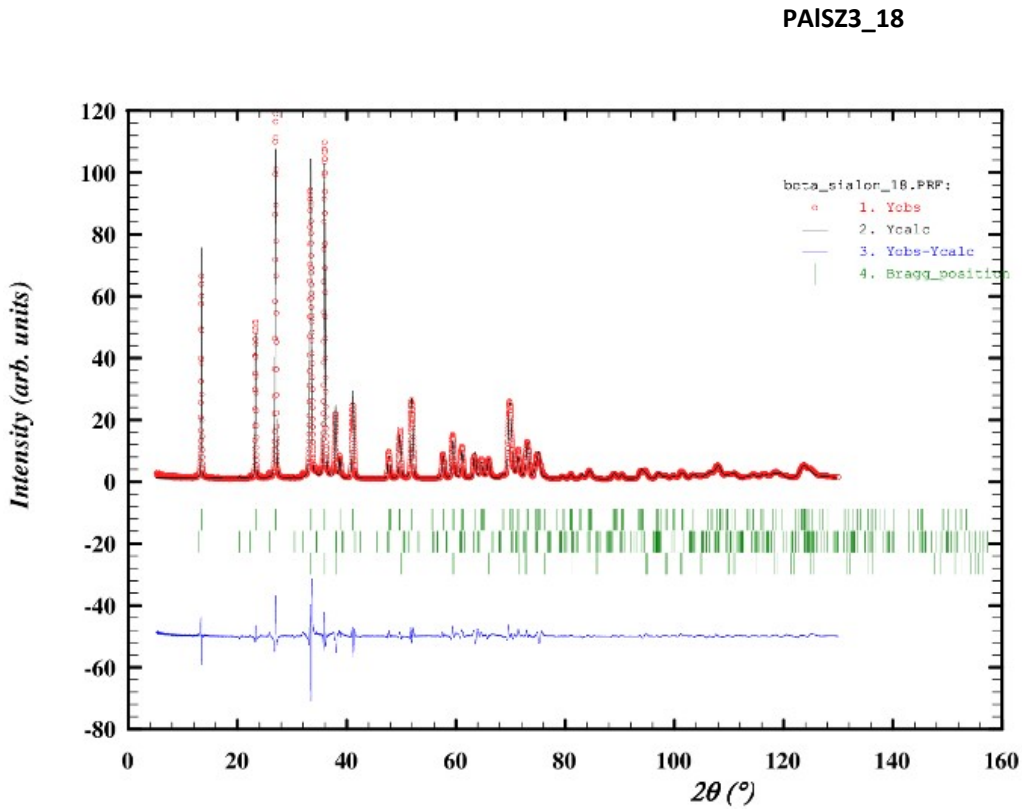


**Figure 6SI.** Rietveld refinement of XRD patterns of **PAlSZ3_18**. *Observed (crosses) and calculated (red line) XRD patterns. Green vertical lines indicate positions of Bragg reflections. Blue line represents difference plot (observed - calculated) on the same scale.*

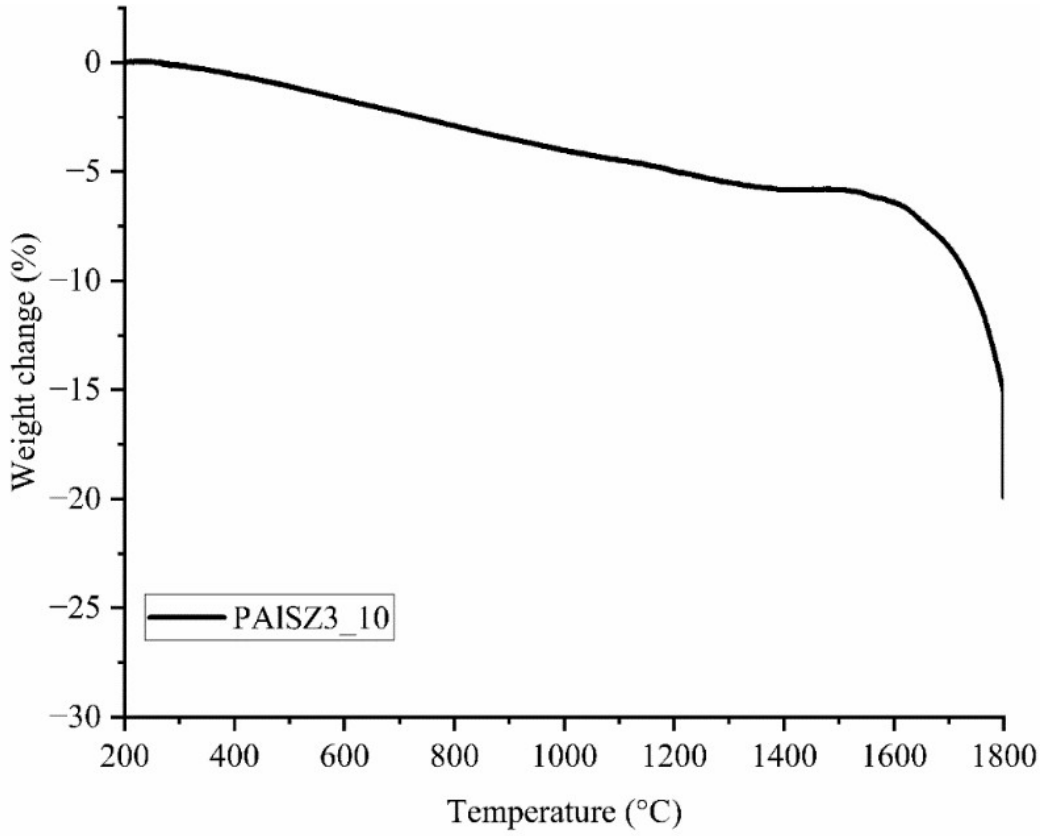


**Figure 7SI.** High-temperature TG analysis of the **PAlSZ3_10**.

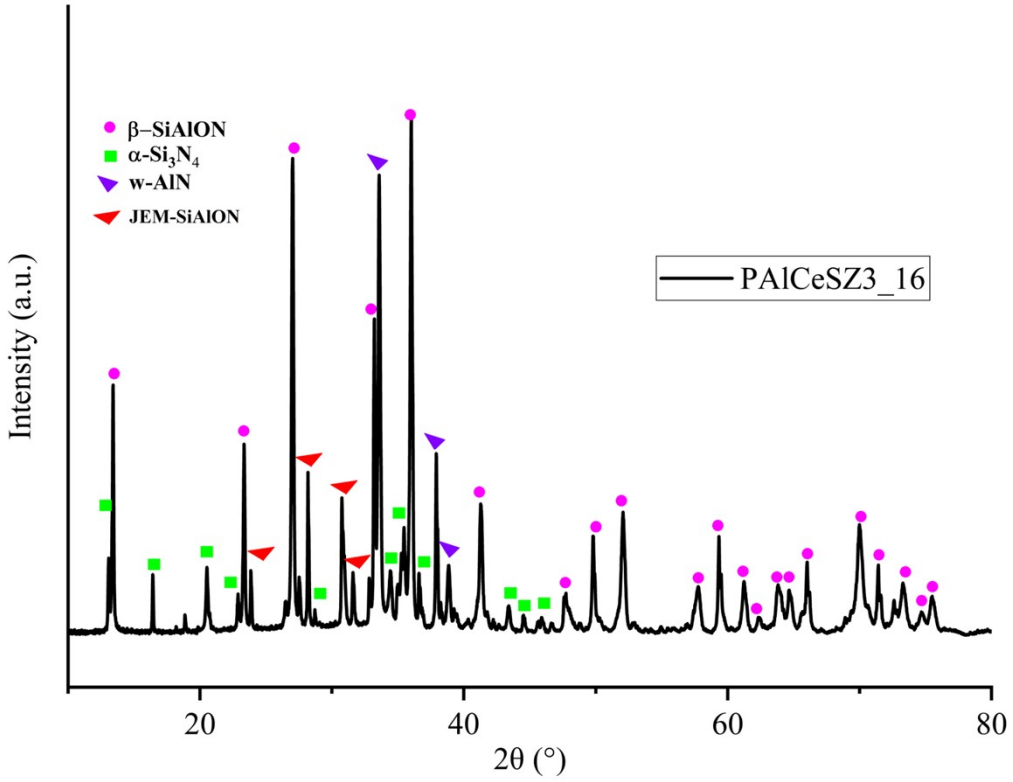


**Figure 8SIa.** X-ray diffraction of **PAlCeSZ3_16**.

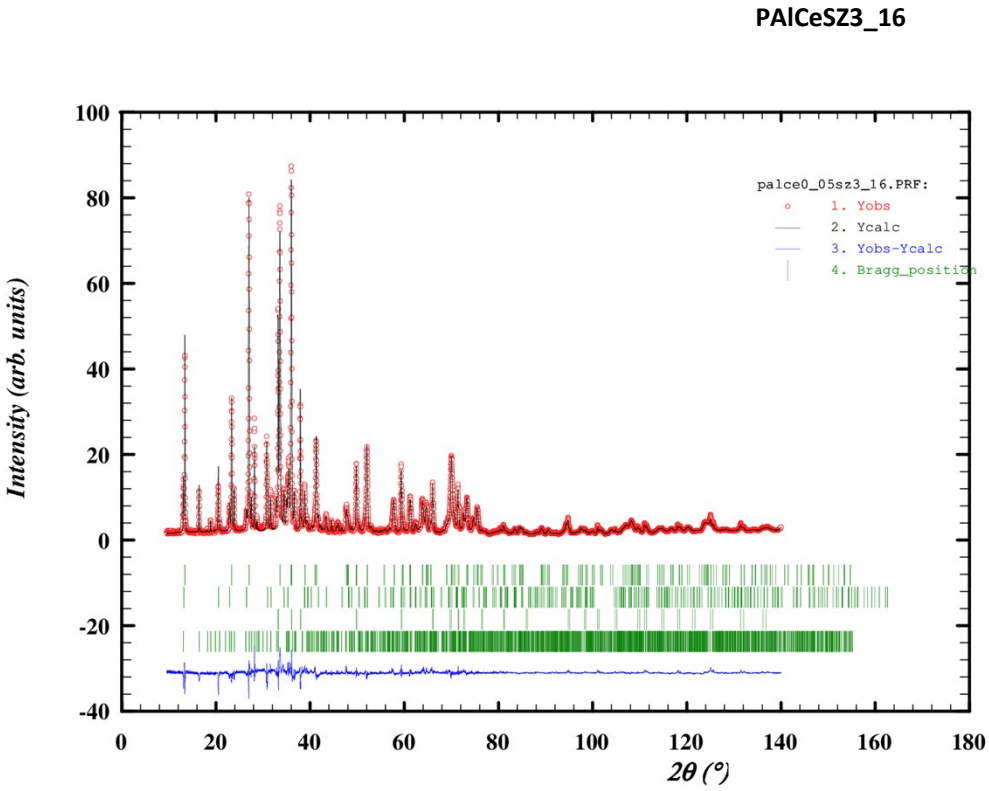


**Figure 8SIb.** (a) XRD patterns of **PAlCeSZ3_16**, (b) Rietveld refinement of the XRD pattern of **PAlCeSZ3_16**. *Observed (crosses) and calculated (red line) XRD patterns. Green vertical lines indicate positions of Bragg reflections. Blue line represents difference plot (observed/calculated) on the same scale. The refined parameters were scale factors, background, sample positioning error, and cell parameters. The overall fit quality results in relatively poor figures of merit ($R_p$ = 10.4 %, $R_{wp}$ = 11.6 %, $R_{exp}$ = 1.9 % and GofF = 5.9). Note that in the Rietveld refinement the model used for JEM phase was based on Ce cation instead of La based JEM phase as proposed in literature.*

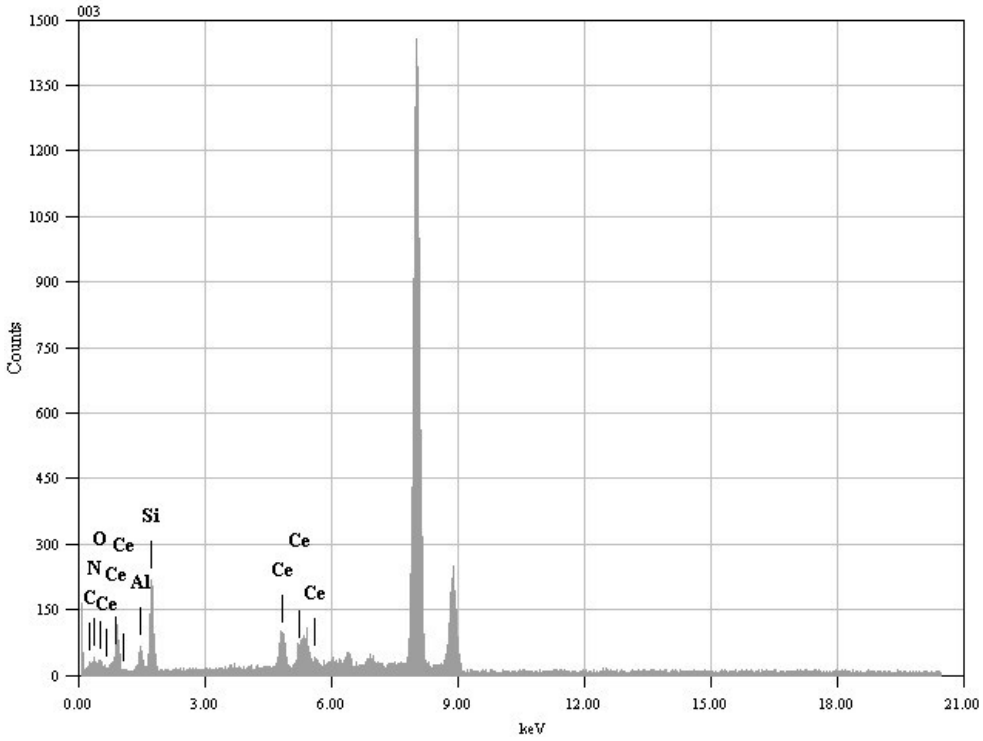


**Figure 9SI.** EDS spectrum of **PAlCeSZ3_GPS18**.

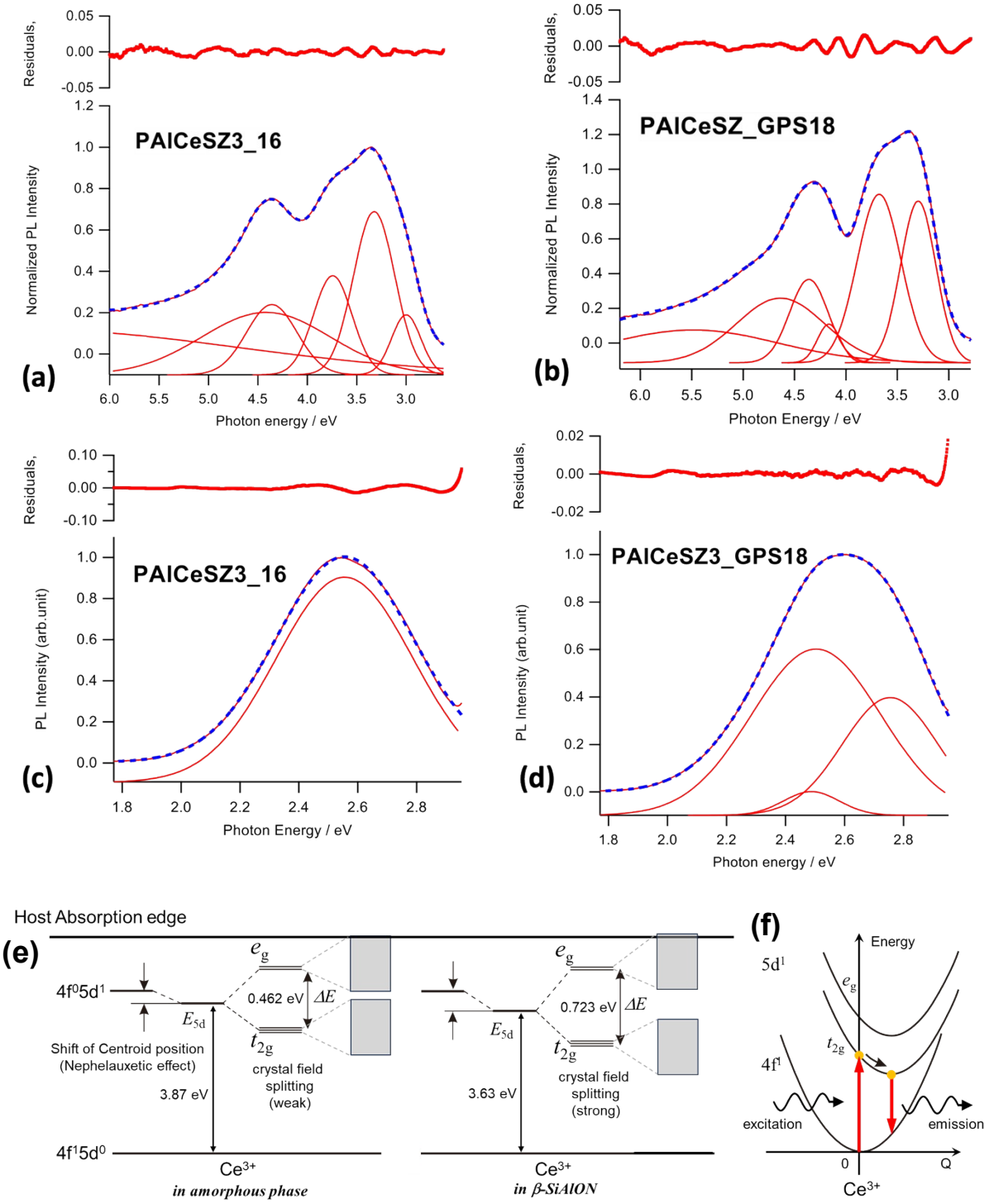


**Figure 10SI.** Photoexcitation (a, b) and emission (c, d) of **PAlCeSZ3_16** and **PAlCeSZ3_GPS18** samples. (e) Energy diagram of $Ce^{3+}$ ions in different crystal fields and relation with band structure and (f) an illustration of the coordination model.

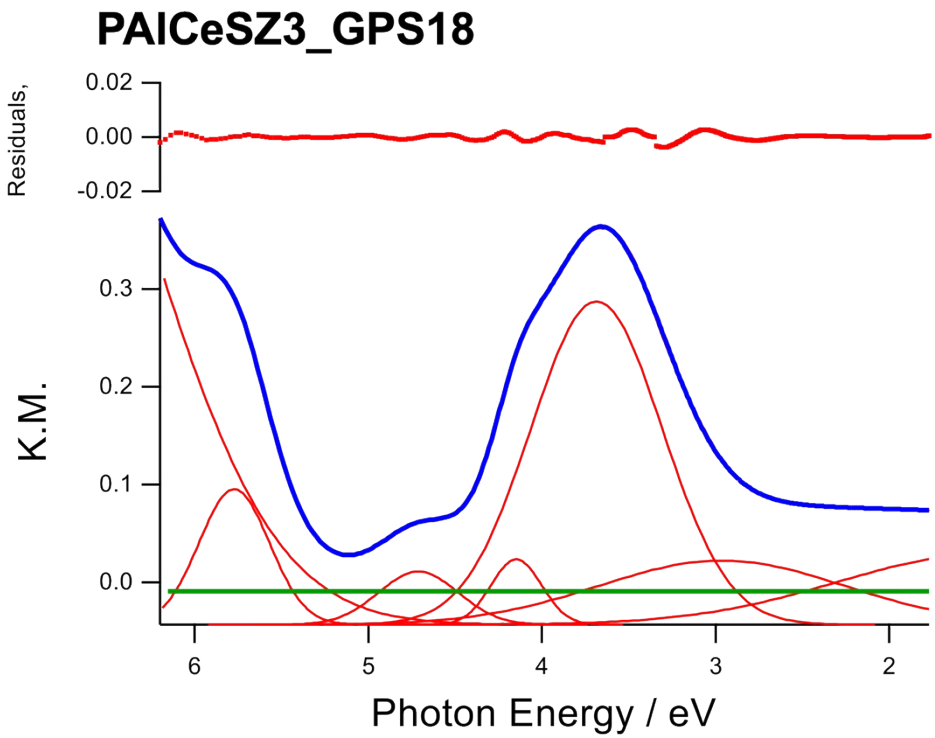


**Figure 11SI.** Optical absorption spectra of the **PAlCeSZ3_GPS18** sample, for band gap analysis and crystal field splitting evaluation.

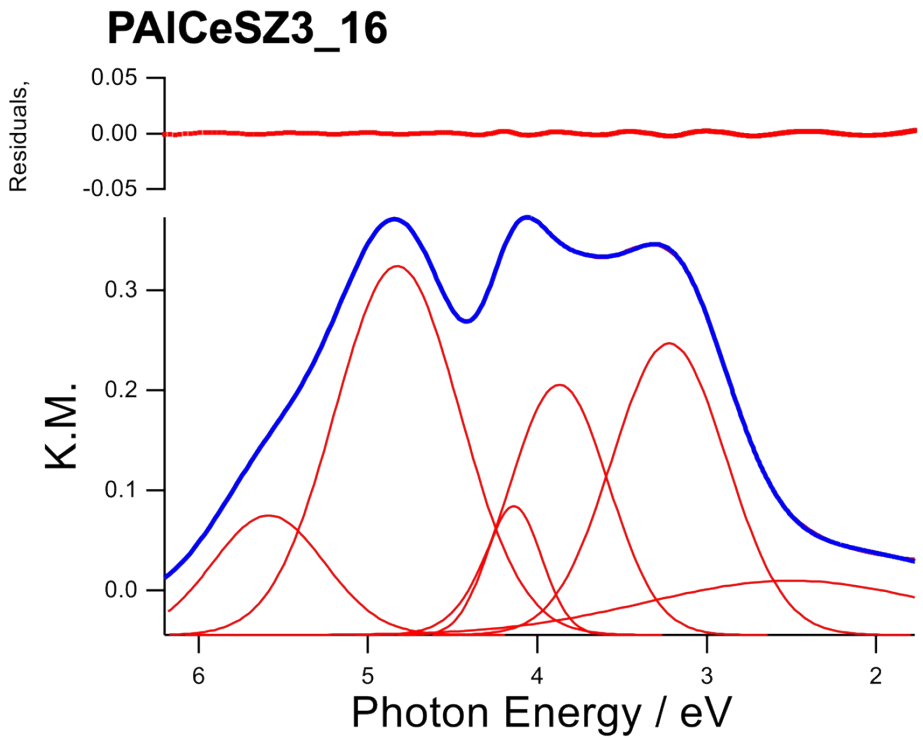


**Figure 12SI.** Optical absorption spectra of the **PAlCeSZ3_16** sample, for band gap analysis and crystal field splitting evaluation.

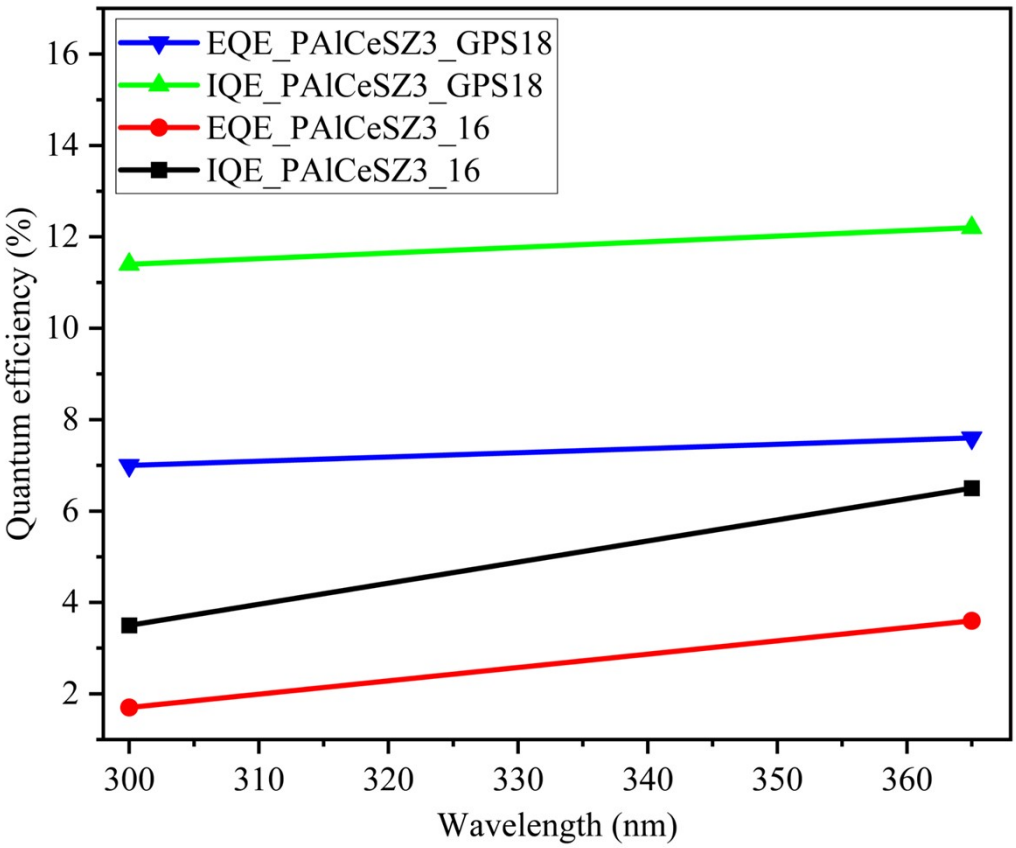


**Figure 13SI.** Internal and external quantum efficiency of **PAlCeSZ3_16** and **PAlCeSZ3_GPS18**.

**Table 1SI.** Phase compositions and cell parameters of the **PAlSZ3_18** sample as determined by Rietveld refinement.

| Parameters | β-SiAlON | α-$Si_3N_4$ | w-AlN |
|---|---|---|---|
| **Crystallite size (nm)** | - | - | - |
| **Strain (%)** | 0.093(4) | - | - |
| ***a*, *b* (Å)** | 7.628(4) | 7.788* | 3.109(2) |
| ***c* (Å)** | 2.930(2) | 5.676* | 4.992(2) |
| **Cell volume (Å$^3$)** | 147.677(8) | 298.18(1) | 41.797(4) |
| **Phase fraction (%)** | 77.6(1) | 0.70(6) | 21.7(8) |

**Table 2SI.** Phase compositions and cell parameters of the **PAlCeSZ3_16** as determined by Rietveld refinement.

| Phase parameters | β-SiAlON | α-$Si_3N_4$ | w-AlN | JEM SiAlON |
|---|---|---|---|---|
| ***a*, *b* (Å)** | 7.617(2) | 7.766(6) | 3.112(2) | 9.396(4), 9.745(4) |
| ***c* (Å)** | 2.915(4) | 5.663(2) | 4.982(2) | 8.927(6) |
| **Cell volume (Å$^3$)** | 146.53(4) | 294.87(2) | 41.79(2) | 817.42(6) |
| **Phase fraction (%)** | 54.7(4) | 13.1(1) | 17.4(1) | 15.1(1) |

**Table 3SI.** Phase compositions and cell parameters of the **PAlCeSZ3_GPS** as determined by Rietveld refinement.

| Phase parameters | β-SiAlON |
|---|---|
| ***a*, *b* (Å)** | 7.637(8) |
| ***c* (Å)** | 2.935(4) |
| **Cell volume (Å$^3$)** | 148.264(2) |

**Table 4SI.** PL quantum yield (PLQY) of the **PAlCeSZ3_16** and **PAlCeSZ3_GPS18**. * Predicted from PLQY at 365 nm excitation, K.M. and PLE data.

| | **PAlCeSZ3_16** | | | **PAlCeSZ3_GPS18** | | |
|---|---|---|---|---|---|---|
| $\lambda_{ex}$ / nm | 300 | 365 | 405* | 300 | 365 | 405* |
| QY internal (%) | 3.4 | 5.7 | 4.6 | 11.4 | 12.2 | 6.1 |
| QY external (%) | 1.8 | 3.4 | 2.4 | 7.0 | 7.6 | 2.0 |